THE ASTROPHYSICAL JOURNAL, 338:296–307, 1989 March 1

VARIABILITY OF X-RAY EMISSION FROM OB STARS

A. COLLURA
Istituto per le Applicazioni Interdisciplinari della Fisica, Palermo

S. SCIORTINO, S. SERIO, AND G. S. VAIANA[1]
Osservatorio Astronomico di Palermo

F. R. HARNDEN, JR.
Harvard-Smithsonian Center for Astrophysics

AND

R. ROSNER
Department of Astronomy and Astrophysics, and Enrico Fermi Institute, The University of Chicago
Received 1987 September 2; accepted 1988 July 19

ABSTRACT

We have studied the variability in soft X-ray emission of 12 OB stars using data obtained with the Imaging Proportional Counter (IPC) of the *Einstein Observatory*. We have analyzed a total of 38 data sections typically of few kiloseconds each. For five of the stars in the sample, combined observations with effective exposure time in the 10–65 ks range (made up of several consecutive few kilosecond data sections) were available. In these five cases the combined observation was also analyzed as a whole.

We have used two different methods of analysis, one more suitable for detecting short-term (typically on time scales <2 ks) variations, the other one, based on comparing count rates evaluated in different data sections, aimed at detection of long time-scale variations (from ~ 2 ks up to months). Both methods have been applied to all stars in our sample.

The long-term variability analysis has shown that Cyg–OB2 8A, ζ Pup, and δ Ori exhibit significant (above the 4 σ significance level) count rate variations between different data sections. Similar variations have been marginally (slightly above the 3 σ significance level) detected also in 15 Mon. The count rate variations between data sections of the other eight stars are consistent with statistical fluctuations. The light curve of Cyg–OB2 8A, the star with the best statistics and coverage in our sample, suggests the existence of two different emission levels; the emission at each level lasts hundreds of kiloseconds. The data available for both the other variable and constant stars in the sample are not incompatible with a similar variability pattern.

The short-term variability analysis has detected marginal variability (slightly above the 3 σ significance level) in τ Sco with an effective amplitude of $\sim 30\%$ and a time scale of ~ 50 s. The upper limits to the effective short-term variability amplitude for all other stars in the sample are in the range $\sim 10\%$–30%. Implications for models of soft X-ray emission from OB stars are also briefly considered.

Subject headings: stars: early-type — stars: variables — stars: X-rays

I. INTRODUCTION

Imaging observations of early-type stars have shown that these stars are X-ray emitters at levels of $\sim 10^{30}$–10^{33} ergs s^{-1} (Harnden *et al.* 1979; Long and White 1980; Vaiana *et al.* 1981; Seward *et al.* 1979; Seward and Chlebowski 1982; Cassinelli *et al.* 1981; Chlebowski, Harnden, and Sciortino 1988). Preliminary spectral analysis had indicated that their emission is consistent with thermal bremsstrahlung (Harnden *et al.* 1979; Cassinelli *et al.* 1981), with typical temperatures ranging between 10^6 and 10^7 K. Further observations have strongly indicated the presence of emission lines at ~ 2 keV, hinting at a wide temperature distribution of the emission measure (Cassinelli and Swank 1983). It is clear that, unless this hot plasma is somehow confined around the star, it will rapidly escape (since the mean thermal velocity far exceeds the surface escape speed of these early-type stars). This confinement may be either inertial (as, for example, in the vicinity of a shock) or magnetic (as, for example, in the coronal "loop" atmosphere associated with the Sun). In any case, one is led to ask how stable such confinement can be and hence to investigate the variability of the observed (X-ray) emission. Such variability analysis are useful in forming (and distinguishing between) models and in constraining the physical parameters of the emitting regions.

Data collected with the *Einstein Observatory* (Giacconi *et al.* 1979) have already been used to investigate this problem. For example, Snow, Cash, and Grady (1981) have reported *Einstein* Imaging Proportional Counter (IPC) observations showing long-term (e.g., few days or more) variability in the O9V star 15 Mon (with a statistical significance of $\sim 5\ \sigma$), in the O9.5II star δ Ori and in the O9III star ι Ori (both with a statistical significance of $\sim 3\ \sigma$); four other stars analyzed by them did not show any similar evidence of variability in their X-ray emission. Cassinelli *et al.* (1983) have searched for X-ray variability in κ Ori and ϵ Ori. Their analysis method involved a χ^2 test for source constancy, but they found no evidence for short-term variability at the 90% significance level.

The analysis of the UV spectra of early-type stars has also shown the presence of short-term variations; for example, hourly variations in the O VI P Cygni profile of the stars δ Ori, ι Ori, and ζ Pup have been reported and interpreted as

[1] Also Harvard-Smithsonian Center for Astrophysics, Cambridge, MA.

evidence of O VI absorption in the stellar wind (York *et al.* 1977); transient ultraviolet narrow absorption components have been reported in the stars ϵ Per (Vidal-Madjar *et al.* 1983), ι Ori, δ Ori, and α Vir and have been interpreted as ejection of matter due to sudden increase of the mass-loss rate (Gry, Lamers, and Vidal-Madjar 1984). Prinja and Howart (1986), using a sample of 21 OB stars, have shown that all ultraviolet discrete absorption components formed in the stellar wind are variable on time scales of the order of hours (see the extensive review of Henrichs 1988).

In this paper we report an analysis of a large sample of data of early-type stars observed with the *Einstein Observatory* IPC using the finalized IPC data analysis software (Harnden *et al.* 1984). We have searched for both long-term and short-term variability. For the long-term variability analysis we used a standard χ^2 test for comparing count rates obtained in different data sections; the short-term variability was studied using a technique recently developed by Collura *et al.* (1987) which allows one to estimate effective variability amplitudes and time scales. For comparison, we have also applied to our data two well-known bin-free variability tests, namely the Kolmogorov-Smirnov test and the Smirnov-Cramer–Von Mises test (see Eadie *et al.* 1971). We have also taken advantage of the moderate energy resolution provided by the IPC in order to examine variability as a function of photon energy; this is in principle important because photon energy discrimination in the variability analysis allows one to distinguish between models for the variability, viz., between intrinsic variations in the stellar emission, and variations in the absorption properties of the intervening gas (viz., the massive stellar wind).

Our paper is structured as follows. In § II, we describe the data and method of analysis; in § III, we present the results of our variability analysis; in § IV, we discuss their implications.

II. THE DATA AND THE METHODS OF VARIABILITY ANALYSIS

a) Data Selection and Analysis

The data used in our variability analysis were obtained with the *Einstein Observatory* IPC (Gorenstein, Harnden, and Fabricant 1981). The moderate energy resolution of the IPC allowed us to study the variability of the emitted radiation both within the entire IPC bandpass, i.e., the "total band" (0.2–4.5 keV), and within two distinct subbandpasses, defined as the "soft band" (0.2–0.8 keV) and the "hard band" (0.8–4.5 keV). Our analysis has been applied separately to each of these three energy bands for every source in our sample. The possible influence of IPC gain variations has been minimized by using the PI (pulse-height independent) rather than the PH (pulse height) value for determining the photon energy, as carried out in the finalized processing of the IPC data (Harnden *et al.* 1984).

The sources were selected so as to ensure a sufficient number of counts to allow meaningful variability analysis with the $\bar{\chi}^2$ method of Collura *et al.* (1987), i.e., we considered those observations in which at least 200 IPC counts were collected. We have therefore selected those observations of OB stars satisfying this criterion from the sample of early-type stars in the Center for Astrophysics *Einstein Observatory* stellar survey (Vaiana *et al.* 1981), and from the Snow, Cash, and Grady (1981) list of OB stars which have been analyzed for long-term variability using an early version of the *Einstein* data analysis software.

With the above criterion, we have included 12 stars in our analysis: ι Ori, ϵ Ori, ζ Pup, α Vir, τ Sco, ζ Oph, ζ Ori, δ Ori, 15 Mon, and the stars 5, 8A, and 9 for the Cyg–OB2 association. Each source observation is denoted by a so-called "sequence number," and is, in general, segmented into consecutive data sections separated by gaps during which useful data could not be collected because of source occultation by the Earth, crossing the South Atlantic Anomaly, drop of telemetry, loss of aspect or high instrumental background. For the above reason, the exposure time (i.e., the time during which useful data could be collected) is in general shorter than the observation duration. The background-subtraced count rates for each star in each of the separate observing sections studied are given in Table 1, together with relevant information on the observations. Count rates and background have been computed using a "local background determination" procedure similar to that adopted in the standard final processing (Harnden *et al.* 1984, 1989). This method, which compares the counts falling in a cell of 2.4 × 2.4 centered at the source position with those falling in a concentric cell 4.0 × 4.0 for hard and total energy bands (for the soft energy band the inner and outer cells are 4.0 × 4.0 and 6.7 × 6.7, respectively) allows one to evaluate source and background counts, their errors, and the source statistical significance in term of the signal-to-noise ratio (for more details, see Harnden *et al.* 1984, 1989). Dead-time, cell size, and vignetting corrections have been applied in deriving the quoted count rates. Note that the use of a larger cell for the soft energy band, dictated by the energy dependence of the IPC point response function, implies that counts in the soft and hard energy bands do not add up exactly to those of the total energy band. The counts used in the short-term analysis were collected as in the standard *Einstein* reduction system in a circular cell of 3′ radius for all three energy bands. In all cases, the finalized *Einstein* IPC analysis software we used rejects observational intervals with anomalously high background.

In five cases (ϵ Ori, τ Sco, and the three Cyg–OB2 stars in our sample), long observations, consisting of several contiguous data sections were available (see Figs. 1–4). In the case of ϵ Ori, and additional observation obtained $\sim$1 month later was also available; in many of the remaining cases, we examined three or four observations separated by days or weeks (each of these observations lasting $\sim$2 ks). In the case of ζ Ori, the available data consist of only one $\sim$2 ks interval.

Due to this heterogeneity of the data, we shall distinguish in the following between short-term variability (which we define as that variability confined to time scales up to the duration of a single observational data section typically less than 3 ks) and long-term variability (which we define as variations in the average flux between observational data sections). Table 1 summarizes the data available for each source in our sample, and the corrected mean count rate in each of the three energy bands in which the data were sorted, namely, the soft (0.2–0.8 keV), hard (0.8–4.5 keV), and total (0.2–4.5 keV) bands.

b) Short-Term Variability Analysis

The low count rate of the sources in our sample and the frequent observational gaps have induced us to limit our analysis to the so-called hypothesis testing methods. These methods can be divided into two categories: bin-free tests and binned tests.

Bin-free tests have the advantage of using the data as they are, but do not allow one to derive parameters of the variable source; they simply test for the presence or absence of variability to some given confidence limit. In our work, we have used

TABLE 1

SUMMARY OF DATA INTERVALS AND MEAN COUNT RATES

STAR NAME AND SEQUENCE NUMBER	START TIME			NET EXPOSURE TIME (s)	MEAN COUNT RATE[a] (s^{-1})		
	Year	Day	U.T.		Soft[b]	Hard[c]	Total[d]
δ Ori (O9.5II)							
I 5100	1980	063	21 36	1416	0.380	0.255	0.470
I 5101	1980	065	05 59	1660	0.377	0.204	0.417
I 5102	1980	083	07 44	1755	0.272	0.185	0.339
I 10414	1981	047	14 35	2610	0.481	0.223	0.466
ϵ Ori (B0I)							
I 5047 (combined)	1980	061	15 07	10360	0.230	0.159	0.289
Section 1		...		2499	0.221	0.165	0.290
Section 2		...		2436	0.242	0.160	0.297
Section 3		...		2253	0.246	0.169	0.308
Section 4		...		1761	0.232	0.149	0.279
Section 5		...		1411	0.195	0.144	0.254
I 3128	1980	085	22 43	1788	0.241	0.163	0.299
ι Ori (O9III)							
I 5095	1980	065	07 26	1821	0.352	0.218	0.417
I 5096	1980	083	01 17	2088	0.406	0.184	0.413
I 10413	1981	047	20 56	2621	0.375	0.156	0.367
ζ Ori (O9.5Ibe + B0III)							
I 2221 (combined)	1979	251	20 46	1854	0.303	0.213	0.384
Section 1		...		765	0.305	0.189	0.361
Section 2		...		1090	0.301	0.230	0.399
ζ Pup (O4I)							
I 5110	1979	324	12 34	1567	0.321	0.384	0.565
I 5111	1979	325	01 22	1977	0.303	0.343	0.514
I 5112	1979	326	07 12	1229	0.145	0.303	0.385
I 5113	1979	328	14 01	1966	0.124	0.302	0.372
α Vir (B1V + B7)							
I 2230	1979	007	18 37	2238	0.176	0.026	0.125
I 4982	1980	017	06 06	1199	0.271	0.052	0.205
ζ Oph (O9V)							
I 5103	1980	061	12 51	2142	0.059	0.065	0.099
I 5104	1980	063	11 26	1925	0.036	0.081	0.102
I 5105	1980	066	05 26	1706	0.058	0.075	0.108
τ Sco (B0V)							
I 831 (combined)	1981	038	07 43	6831	0.320	0.358	0.540
Section 1		...		1311	0.334	0.360	0.548
Section 2		...		860	0.380	0.399	0.613
Section 3		...		954	0.318	0.317	0.496
Section 4		...		1311	0.330	0.382	0.568
Section 5		...		699	0.316	0.314	0.492
Section 6		...		1679	0.279	0.367	0.525
15 Mon (O7Vf)							
I 5088	1980	080	01 22	940	0.116	0.123	0.188
I 5089	1980	085	06 08	2125	0.072	0.059	0.087
I 5090	1980	102	00 12	1508	0.069	0.051	0.090
Cyg-OB2 5 (O7Ianfp + O6f)							
I 4221 (combined)	1980	161	13 06	65463	0.026	0.106	0.121
Section 1		...		5136	0.027	0.110	0.125
Section 2		...		4355	0.030	0.099	0.117
Section 3		...		8688	0.020	0.105	0.117
Section 4		...		9356	0.021	0.105	0.117
Section 5		...		10478	0.027	0.106	0.121
Section 6		...		8264	0.027	0.107	0.122
Section 7		...		4081	0.030	0.098	0.114
Section 8		...		12161	0.030	0.102	0.125
Section 9		...		2764	0.028	0.123	0.139

TABLE 1—*Continued*

Star Name and Sequence Number	Start Time			Net Exposure Time (s)	Mean Count Rate[a] (s^{-1})		
	Year	Day	U.T.		Soft[b]	Hard[c]	Total[d]
Cyg–OB2 8A (O6Ib)							
I 4221 (combined)	1980	161	13 06	65463	0.045	0.143	0.168
Section 1		...		5136	0.053	0.191	0.221
Section 2		...		4355	0.043	0.199	0.223
Section 3		...		8688	0.059	0.171	0.204
Section 4		...		9356	0.038	0.122	0.144
Section 5		...		10478	0.041	0.125	0.148
Section 6		...		8264	0.057	0.135	0.167
Section 7		...		4081	0.032	0.124	0.142
Section 8		...		12161	0.040	0.125	0.147
Section 9		...		2764	0.038	0.155	0.177
Cyg–OB2 9 (O5I+)							
I 4221 (combined)	1980	161	13 06	65463	0.006	0.035	0.038
Section 1		...		5136	0.003	0.036	0.037
Section 2		...		4355	0.002	0.042	0.043
Section 3		...		8688	0.008	0.033	0.037
Section 4		...		9356	0.006	0.030	0.033
Section 5		...		10478	0.011	0.037	0.043
Section 6		...		8264	0.004	0.042	0.044
Section 7		...		4081	0.000	0.032	0.031
Section 8		...		12161	0.009	0.029	0.034
Section 9		...		2764	0.004	0.040	0.042

[a] Errors on the quoted count rates can be estimated using Poisson statistics: the total number of counts is given by the mean count rate times the net exposure (the background can be neglected in these strong sources), the statistical error on the number of counts is its square root and dividing it by the net exposure gives the statistical error on the count rate. Systematic errors are negligible with respect to statistical errors.

[b] Soft: (0.2–0.8) keV bandpass.

[c] Hard: (0.8–4.5) keV bandpass.

[d] Total: (0.2–4.5) keV bandpass.

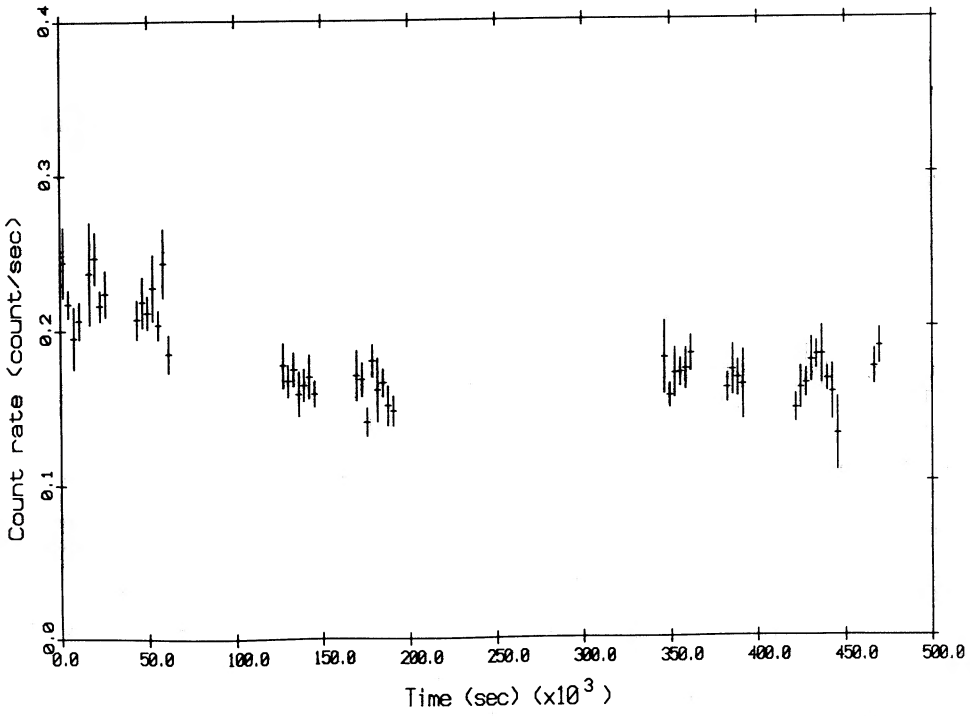

FIG. 1.—IPC count rate light curve of Cyg–OB2 8A showing long-term variability. The data refer to the 0.2–4.5 KeV energy band and are binned in 3000 s intervals; the time axis origin is the start of the observation. Several small gaps (shorter than binning intervals) reduced the net exposure time to the value of ~65 ks.

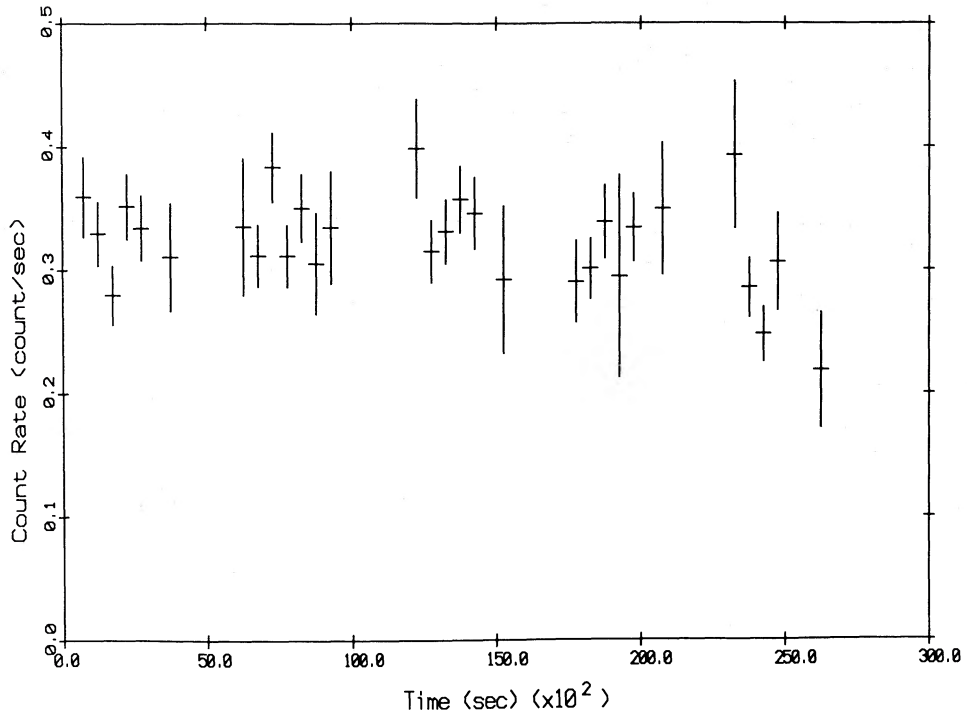

FIG. 2.—IPC count rate light curve of ϵ Ori (sequence No. 5047). The data refer to the 0.2–4.5 keV energy band and are binned in 500 s bins; the time axis origin is the start of the observation.

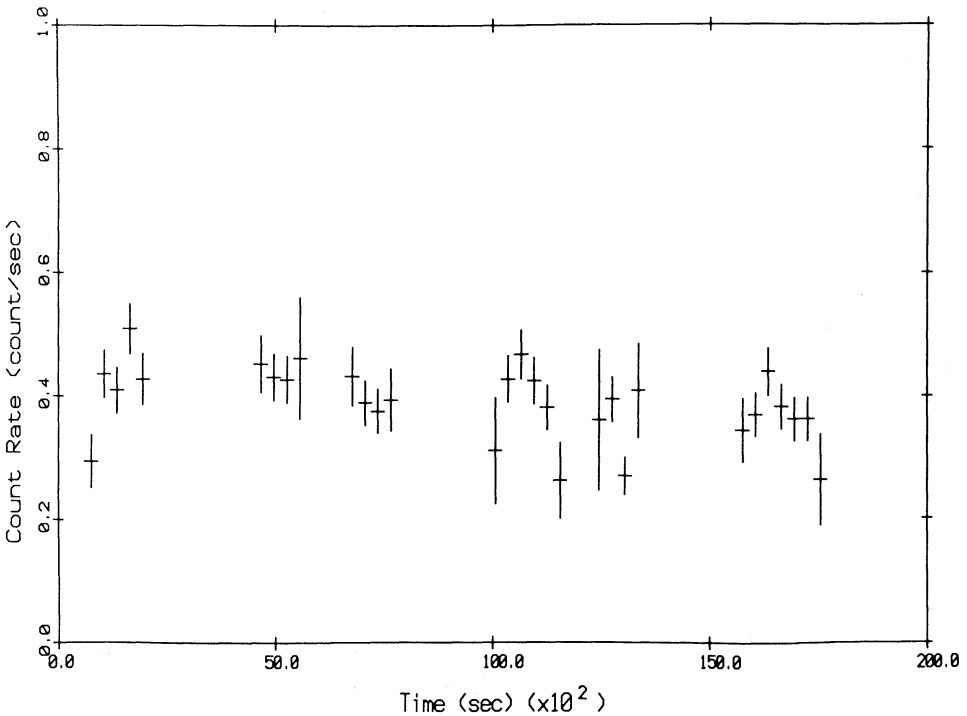

FIG. 3.—IPC count rate light curve of τ Sco. The data refer to the 0.8–4.5 keV energy band and are binned in 300 s bins; the time axis origin is the start of the observation.

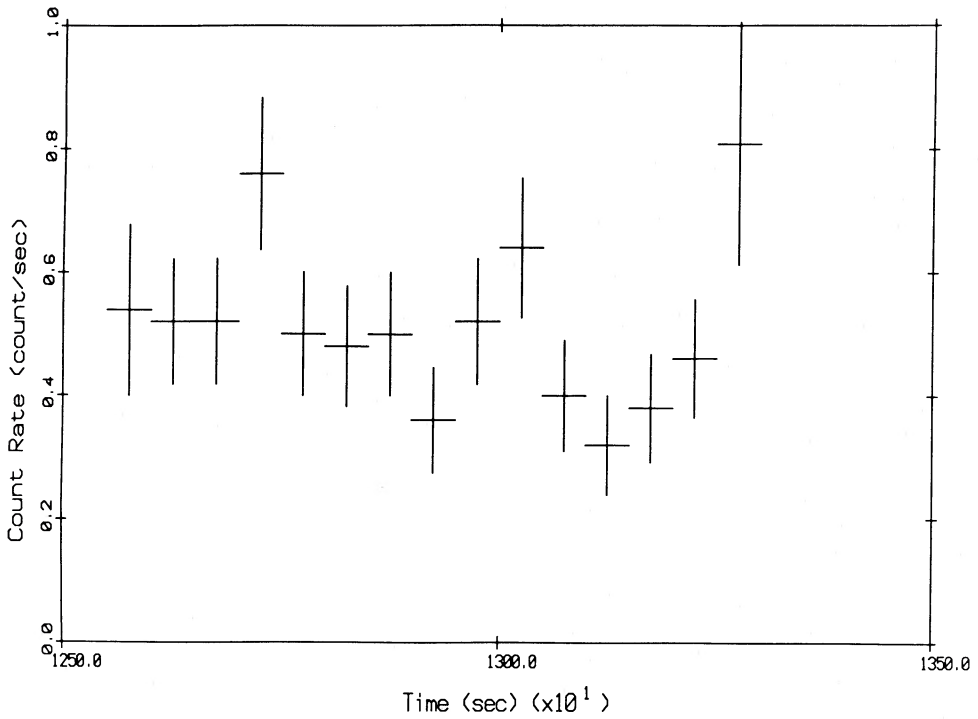

FIG. 4.—IPC count rate light curve of τ Sco during the fifth data section where marginal variability has been detected. The data refer to the 0.2–4.5 keV energy band and are binned in 50 s bins.

the Kolmogorov-Smirnov (KS) and the Smirnov-Cramer–Von Mises (NW^2) tests (see Eadie *et al.* 1971) as a supplement and verification of our $\bar{\chi}^2$ test described below, and found consistent results in all cases.

The binned tests have the advantage of allowing one to estimate the source's variability parameters (for example, variability amplitude and time scale), but usually require manipulation of the data (e.g., binning) which may be arbitrary.

In the main part of this work we have used a binned method of analysis (the "$\bar{\chi}^2$" test), described by Collura *et al.* (1987), that gives results that are essentially independent of the way the binning is performed. In this sense, it resembles the unbinned test, but it allows detection of short-term variability, estimation of pulsed power in the source emission, and identification of the prevalent time scales involved. The detection of variability is model independent whereas estimation of pulsed power and identification of the prevalent time scale are achieved within the context of a specific model for the character of the flux variations (note that this model does not presume a *mechanism* for the variability, but only the functional "shape" of the variable flux component).

Here we briefly summarize the main steps in the application of the $\bar{\chi}^2$ test to the binned data. The photon arrival times are first binned into intervals of duration much smaller than the minimum bin size on which the test will be performed. This latter minimum bin size $\Delta t_{\rm min}$ is fixed by requiring a minimum average of 5 counts per bin. A χ^2 test is performed on the binned data; the phase of the binning is changed several times by simply shifting the starting time $t_{\rm start} \equiv t_0 + \phi\,\Delta t/2\pi$ of the binning, and an effective $\bar{\chi}^2(\Delta t) = \langle \chi^2(\Delta t, \phi)\rangle$, representative of the bin size Δt, is determined by averaging the $\chi^2(\Delta t, \phi)$ values over the binning phases ϕ. The procedure is repeated at several bin sizes Δt, the maximum bin size $\Delta t_{\rm max}$ being dictated by the observation length (at least 3 bins have been used); thus $\Delta t_{\rm min} < \Delta t < \Delta t_{\rm max}$. Variability is detected if at least one of the $\bar{\chi}^2(\Delta t)$'s exceeds a predetermined significance level. The effective variability amplitude is then determined according to a model variable source consisting of a constant source plus a train of randomly spaced, equal-amplitude, square-shaped pulses; this amplitude is given by the expression

$$V_{\rm eff}(\Delta t) = \left\{\frac{n-1}{n}\,\frac{[\bar{\chi}^2(\Delta t) - 1]}{I}\right\}^{1/2}, \qquad (2.1)$$

where n is the number of bins, Δt is the bin duration, and I is the mean number of counts per bin; $V_{\rm eff}(\Delta t)$ is related to the pulse amplitude V_0 by the equation $V_{\rm eff}(\Delta t) = V_0(\Delta t) \times [\delta(1-\delta)]^{1/2}$, where δ is the duty cycle of the variable component. It is straightforward to show that the amplitude of the effective variability as a function of the bin size is almost constant for bin sizes shorter than the variability time scale (i.e., the duration of individual pulses) and decreases rapidly for bin sizes longer than the dominant time scale of variability (Collura *et al.* 1987). The point at which a change in slope of a graph of variability amplitude versus sampling bin size occurs therefore gives an estimate of the dominant characteristic time scale of the variability. A more quantitative estimate of this scale is derived in Collura *et al.* (1987) where it is shown that the time scale is identified by the bin size at which the variability falls below $\sim$86% its maximum value. The error in this estimate depends on the statistical significance of the variability itself, and is generally of the order of a factor of 2 (at the 68% confidence level) for the variable sources of our sample (see Collura *et al.* 1987).

Our procedure was carried out separately in each of the

three energy bands defined above and was applied to data sorted in up to three different ways: (1) Each data section delimited by large data gaps was analyzed; (2) when separate data sections followed one another without large data gaps, such data sections were combined and analyzed (such was the case for ϵ Ori, ζ Ori, τ Sco, and the Cyg-OB2 stars); and (3) each entire observation has been analyzed.

Since the background intensity was in all cases much lower than the intensity of the sources considered here, contamination due to background fluctuations consistent with the counting statistics can be excluded. However, in order to rule out spurious variability which may arise because of variations of the background itself beyond those expected from photon statistics, we have analyzed the short-term variability of the background in the "total band." In all cases, this analysis demonstrated that background variations cannot influence our results.

By defining the mean rate for each observing interval, and then binning as described above, we can also construct graphs of the fractional variability $V_{\rm eff}(\Delta t)$ of each source as a function of the binning interval Δt. In addition, we have constructed fiducial curves which define the 2 σ (95.5%), 3 σ (99.73%) and 4 σ (99.994%) significance levels. In Figures 5–9 we show examples of such variability plots. The bin size at which $V_{\rm eff}(\Delta t)$ falls below 86% its maximum value approximately identifies the variability time scale; and the error in $V_{\rm eff}$ is given by equation (3.14) of Collura *et al.* (1987).

c) *Long-Term Variability Analysis*

We have also performed a search for "long-term" changes in the corrected count rate (or flux) for all sources in our sample observed more than once, and in those sources, namely, ϵ Ori, τ Sco, Cyg–OB2 5, 8A, and 9, whose observations consist of several data sections separated by large gaps. This analysis has been performed separately in the total, hard, and soft energy bands using a standard χ^2 test for source constancy applied to the corrected count rates of Table 1. In those stars showing evidence of significant variability we have evaluated an effective fractional variability,

$$V_{\rm eff} = \frac{[\sum_i (I_i - \bar{I})^2]^{1/2}}{\bar{I}}, \qquad (2.2)$$

where I_i is the source corrected count rate in the ith observation or subsection and $\bar{I}$ is the mean source corrected count rate obtained as the average of the source-corrected count rates weighted by their errors.

III. RESULTS

In this section, we summarize the overall results of our analysis, focusing in detail on results for those sources which show plausible evidence for variability. There are two essential points to our analysis: first, the methods we use to study short-term variability are better suited to the problem than those previously employed (Snow, Cash, and Grady 1981; Cassinelli *et al.* 1983) because repeated binning with varying binning phase is necessary in order to prevent spurious averaging of real fluctuations on the binning time scale (see § II above); second, the final data processing we use gives lower gain uncertainties compared to the data processing used previously, thus resulting in more reliable variability estimates.

It is important to note that because of the large number of

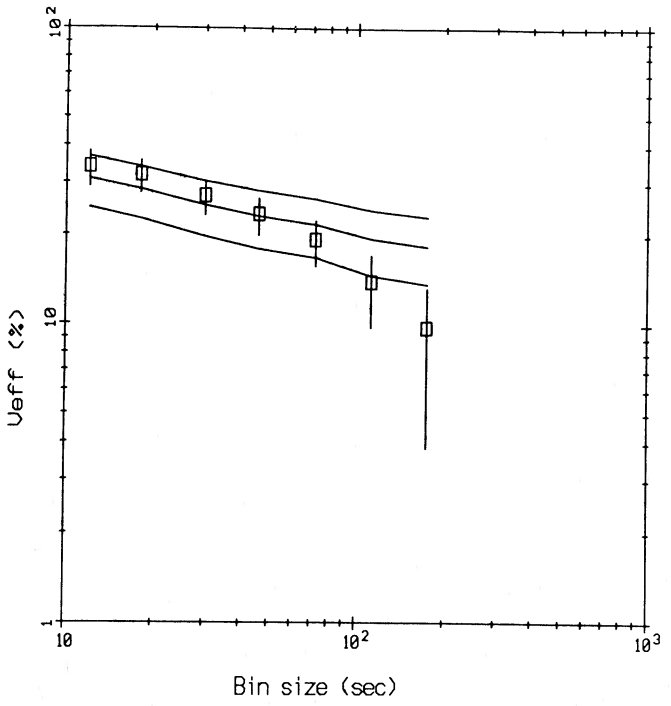

FIG. 5

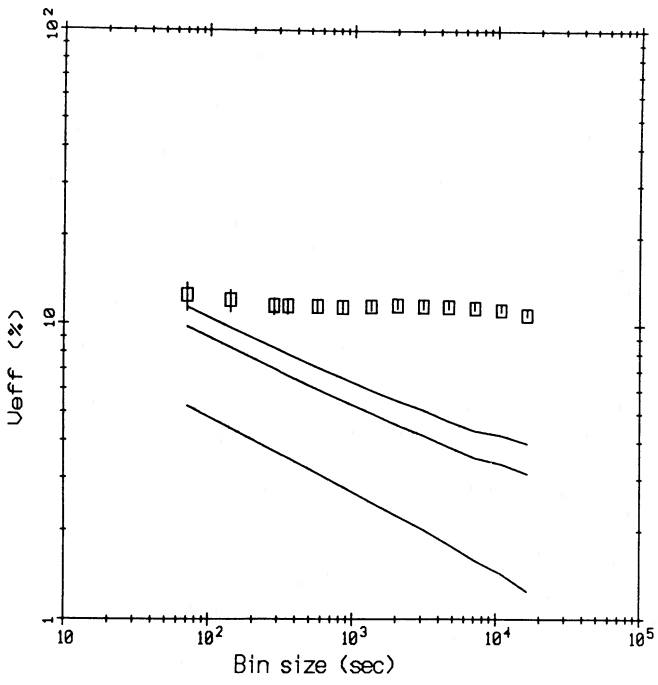

FIG. 6

FIG. 5.—Fractional variability (*open squares*) as a function of bin size for τ Sco (sequence No. 831, fifth interval) in the 0.2–4.5 keV energy band; 1 σ error bars on fractional variability are computed according to eq. (3.14) of Collura *et al.* (1987). Solid lines are the computed 2 σ (95.5%, *lower line*), 3 σ (99.73%), and 4 σ (99.994%, *upper line*) variability significance levels as a function of bin size.

FIG. 6.—Fractional variability (*open squares*) as a function of bin size for Cyg–OB2 8A in the 0.2–4.5 keV energy band; error bars and solid lines are as in Fig. 5

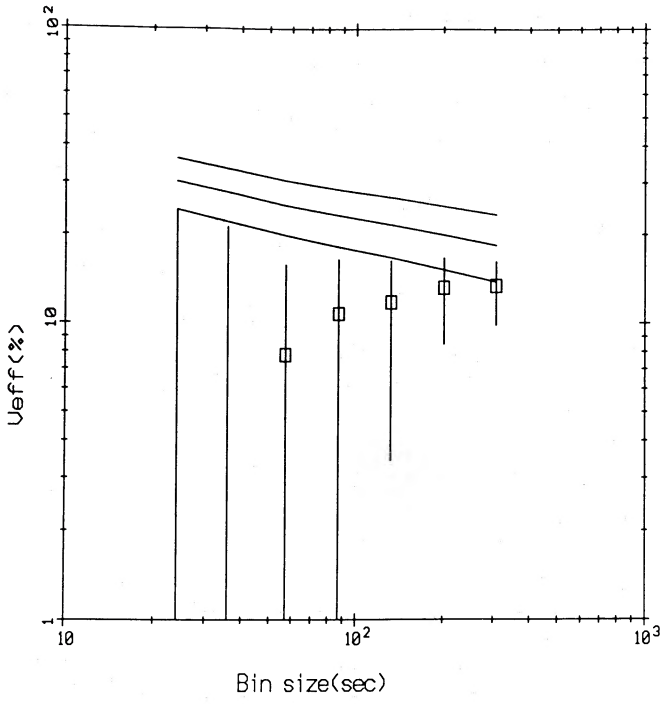

FIG. 7

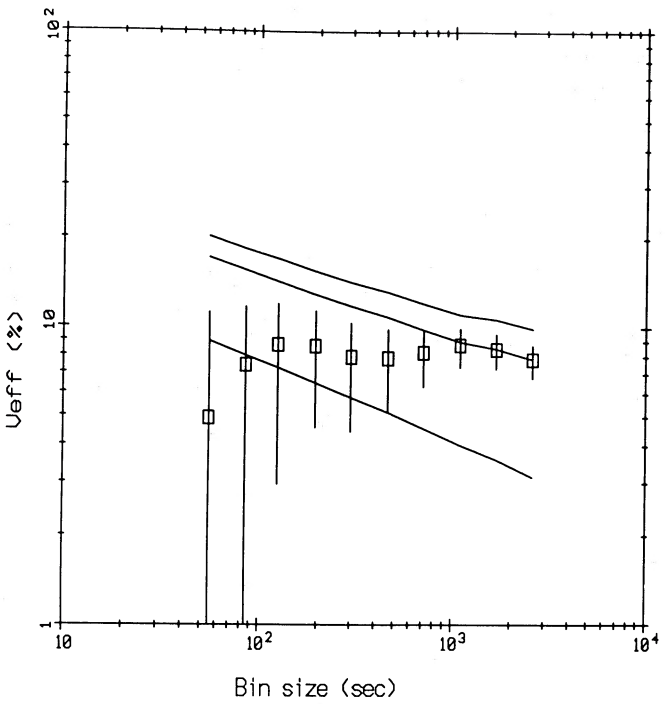

FIG. 8

FIG. 7.—Fractional variability (*open squares*) as a function of bin size for ζ Pup (sequence No. 5112) in the 0.8–4.5 keV energy band; error bars and solid lines are as in Fig. 5.

FIG. 8.—Fractional variability (*open squares*) as a function of bin size for ϵ Ori (sequence No. 5047) in the 0.8–4.5 keV energy band; error bars and solid lines are as in Fig. 5.

data intervals considered, we regard variability detected at the 3 σ (99.73%) level to be marginal; and only regard results obtained at the 4 σ (99.994%) level or higher as significant.

a) Short-Term Variability

We summarize in Table 2 the results of the short-term variability analysis confined to those observational intervals for which the reported variability levels were obtained at the greater than 95% confidence level; we give the results of the $\bar{\chi}^2$ tests [variability significance, value of the effective fractional variability (in percent) with 1 σ errors and variability time scale as derived by the $\bar{\chi}^2$ method]. Variability significance derived through application of KS and NW[2] tests is in good agreement with the $\bar{\chi}^2$ test results. Representative analysis results are

TABLE 2

SUMMARY OF SHORT-TERM VARIABILITY ABOVE THE 95% SIGNIFICANCE LEVEL

STAR NAME AND SEQUENCE NUMBER	SOFT BAND[a]			HARD BAND[b]			TOTAL BAND[c]		
	$P(\bar{\chi}^2)$[d]	V_{eff}[e]	τ[f]	$P(\bar{\chi}^2)$[d]	V_{eff}[e]	τ[f]	$P(\bar{\chi}^2)$[d]	V_{eff}[e]	τ[f]
ϵ Ori (B0I)									
I 5047 (combined)	98.0	16 ± 4	~100	99.69	8 ± 2	≥2500	96	6 ± 2	≥2500
τ Sco (B0V)									
I 831 (combined)	...	...	...	98.6	8 ± 2	1000	...	...	...
Section 5	99.0	35 ± 6	≤50	...	...	...	99.94	30 ± 4	50
Cyg–OB2 5 (O7Ia + O6If)									
I 4212 (combined)	98.5	17 ± 4	600	98.4	5 ± 1	1400	97.5	5 ± 1	1400
Cyg–OB2 8A (O6Ib)									
I 4212 (combined)	99.998	10 ± 2	$>10^4$	≫99.999	13 ± 2	$>10^4$	≫99.999	13 ± 2	$>10^4$

[a] Soft: (0.2–0.8) keV bandpass.
[b] Hard: (0.8–4.5) keV bandpass.
[c] Total: (0.2–4.5) keV bandpass.
[d] $P(\bar{\chi}^2)$ is the statistical significance, in percent, at which we can reject the null hypothesis of constancy.
[e] V_{eff} is the maximum value of the effective variability, in percent, as a function of binning size.
[f] τ is the variability time scale, in second (*see text*).

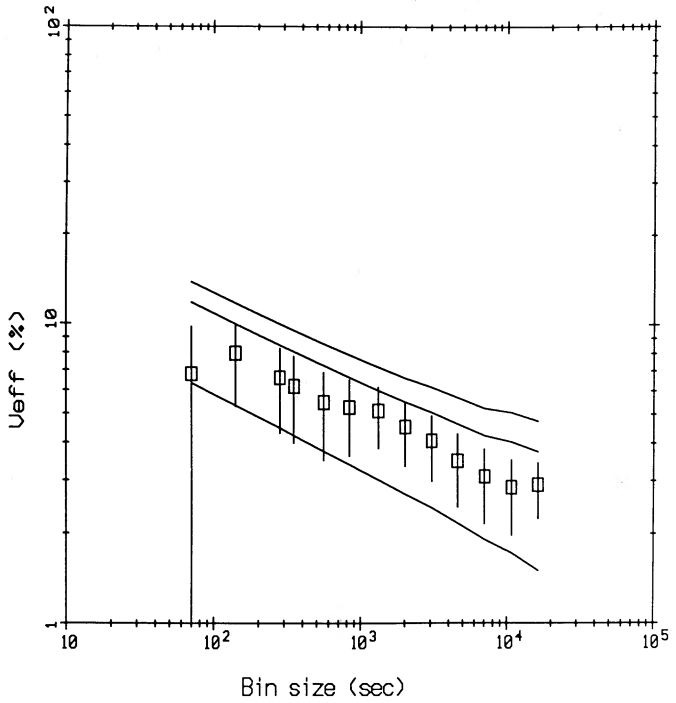

FIG. 9.—Fractional variability (*open squares*) as a function of bin size for Cyg–OB2 5 in the 0.2–4.5 keV energy band; error bars and solid lines are as in Fig. 5.

shown in graphical form in Figures 5–9.

As can be deduced from Table 2, no stars show evidence for short-term variations at very high (say at 5 σ or the 99.99994%) statistical significance level; only τ Sco shows evidence for marginal variability (above the 3 σ level) while there is no evidence for variability in the other stars in the sample. The entire τ Sco observation, lasting $\sim$7 ks and made up of six continuous data sections (Fig. 3) does not show evidence for variability. Its fifth data section (Fig. 4) shows marginal variability (at 99.94% significance level) in the total energy band on a time scale of $\sim$50 s, and with a fractional amplitude of $\sim$30% (see Fig. 5).

For the sake of completeness, we quote in Table 3 upper bounds to short-term fractional variability amplitudes. Since these upper bounds obviously depend on the data binning, we show only 3 σ upper bounds evaluated at a uniform binning duration of 200 s, based on the $\bar{\chi}^2$ analysis method. Note that because variability over time scales larger than the binning interval and shorter than the duration of the observational interval is not filtered out by the binning, the values shown in Table 3 are actually upper limits on variability over time scales ranging from 200 s up to the duration of each observational interval. Since, however, the method sensitivity increases at longer time scales, the quoted upper limits are, strictly speaking, too conservative if variability on time scales longer than 200 s is considered. This can be immediately seen from the solid lines of Figures 5–9 representing the 2, 3, and 4 σ variability amplitude upper limits as a function of the bin size.

TABLE 3

SUMMARY OF SHORT-TERM VARIABILITY UPPER BOUNDS

STAR NAME AND SEQUENCE NUMBER	VARIABILITY AMPLITUDE UPPER BOUNDS (%)			STAR NAME AND SEQUENCE NUMBER	VARIABILITY AMPLITUDE UPPER BOUNDS (%)		
	Soft[a]	Hard[b]	Total[c]		Soft[a]	Hard[b]	Total[c]
δ Ori (O9.5II)				α Vir (B1V + B7)			
I 5100	20	40	18	I 4982	29	53	25
I 5101	19	38	17	I 2230	23	70	22
I 5102	19	39	17				
I 10414	19	34	16	τ Sco (B0V)			
				I 831 (combined)	15	10	8
ϵ Ori (B0I)							
I 5047 (combined)	14	13	9	ζ Oph (O9V)			
I 3128	23	41	20	I 5103	47	33	26
				I 5104	49	32	27
ι Ori (O9III)				I 5105	60	33	29
I 5095	17	19	12				
I 5096	16	19	12	15 Mon (O7Vf)			
I 10413	16	17	12	I 5088	37	50	31
				I 5089	36	55	30
ζ Ori (O9.5Ibe + B0III)				I 5090	40	60	32
I 2221 (combined)	21	17	13				
				Cyg–OB2 5 (O7Ianfp + O6f)			
ζ Pup (O4I)				I 4221 (combined)	23	10	9
I 5110	25	16	14				
I 5111	26	15	13	Cyg–OB2 8A (O6Ib)			
I 5112	22	24	16	I 4221 (combined)	18	9	8
I 5113	18	19	13				
				Cyg–OB2 9 (O5I +)			
				I 4221 (combined)	23	11	10

[a] Soft: (0.2–0.8) keV bandpass.
[b] Hard: (0.8–4.5) keV bandpass.
[c] Total: (0.2–4.5) keV bandpass.

TABLE 4

SUMMARY OF LONG-TERM VARIABILITY ANALYSIS

STAR NAME	SOFT BAND[a]			HARD BAND[b]			TOTAL BAND[c]		
	$P(\chi^2)$[d]	V_{eff}[e]	τ[f]	$P(\chi^2)$[d]	V_{eff}[e]	τ[f]	$P(\chi^2)$[d]	V_{eff}[e]	τ[f]
δ Ori (B0I)	99.998	21	days	96.2	11	days	99.98	13	days
ι Ori (B0I)	...	...	...	99.2	14	weeks	...	...	...
ζ Pup (O4I)	$\gg$99.999	42	days	97.4	10	days	>99.999	18	days
15 Mon (O4I)	...	...	...	99.8	34	days	99.95	33	days
Cyg–OB2 8A (O6Ib)	98.5	19	hr	$\gg$99.999	17	hr	$\gg$99.999	17	hr

[a] Soft: (0.2–0.8) keV bandpass.
[b] Hard: (0.8–4.5) keV bandpass.
[c] Total: (0.2–4.5) keV bandpass.
[d] $P(\chi^2)$ is the statistical significance, in percent, at which we can reject the null hypothesis of constancy on the basis of χ^2 test statistic.
[e] V_{eff} is the value of the effective variability in percent.
[f] τ is the variability time scale.

b) *Long-Term Variability*

In Table 4 we summarize the corresponding results for long-term variability,[2] and again report (as in Table 2) only results with confidence levels above 95%. The quoted variability time scales in this case simply correspond to the typical separation times between the subintervals considered, and therefore should not be regarded as *the* time scales for intrinsic source variations (i.e., the source may also be varying on shorter time scales, but this analysis could not characterize such variations).

In the case of long-term variations, the star 8A of Cyg–OB2 shows variability above the 5 σ (99.99994%) level on a time scale greater than 10^4 s in the hard and total bands. Similar analysis show significant (larger than 4 σ) level variation in the soft band X-ray emission for δ Ori and ζ Pup, and marginal variability (slightly larger than 3 σ) for 15 Mon in the total band.

In the following, we discuss in detail the long-term variability analysis results for Cyg–OB2 8A, ζ Pup, δ Ori, and 15 Mon.

i) Cyg–OB2 8A

We have examined a long observation of Cyg–OB2 8A, spanning $\sim$6 days and accumulating an exposure time of $\sim$65 ks (see Fig. 1). The data consist of a sequence of 75 consecutive (but not always contiguous) intervals. Variability has been detected at a confidence level larger than 99.999% both with the $\bar{\chi}^2$ method and the standard χ^2 long-term variability method (see § II*a*) in the hard and total energy bands (see Fig. 5) and less significantly in the soft band; the soft band statistics is, however, limited by a strong absorption that reduces the number of counts available for the analysis. The $\bar{\chi}^2$ method yields a 10^4 s lower limit to the variability time scale and sets a variability amplitude of $\sim$13%; the comparison of count rates of different data section using the χ^2 long-term variability method indicates that the corrected count rate significantly changes between different data sections and gives an effective variability amplitude of $\sim$17%. The agreement between this value and that found using the $\bar{\chi}^2$ method is reasonably good given the different models underlying the two estimates.

A visual inspection of the light curve in Figure 1 shows that a step function (at $\sim$100 ks) is compatible with the data. Assuming this variability pattern, the $\bar{\chi}^2$ method would yield a time scale which is the duration of the higher emission state; however, the data gaps prevent from extending the analysis to bin sizes larger than $\sim 10^4$ s, which is the variability time scale lower limit quoted in our results. Furthermore, the presence of a long gap between 60 ks and 110 ks hides the actual variability pattern preventing a better characterization of the variability itself.

[2] Note that since different data sections have in general widely different duration, long-term variability amplitude upper limits cannot be derived straightforwardly as for the short-term variability case reported in Table 3.

ii) ζ *Pup*

We have analyzed four distinct observations of ζ Pup separated by 1–3 days intervals and made up of a single data section each. This star shows significant (larger than 4 σ) corrected count rate differences in the soft band (and, with a slightly smaller level of significance, in the total band). The effective variability amplitude is $\sim$42% in the soft band and $\sim$18% in the total band with a time scale of days.

iii) δ *Ori*

We have analyzed four distinct observations of δ Ori made up of a single data section each and separated by intervals ranging from 2 days up to $\sim$1 yr duration. This star shows significant (larger than 4 σ) long-term variability in the soft band count rate (and with a smaller level of significance in the total band). The effective variability amplitude is $\sim$21% with a time scale of days.

iv) *15 Mon*

Three observations made up of a single data section each and taken a few days apart have been analyzed for this star. The analysis suggests marginal (larger than 3 σ) variability in the total band with an amplitude of $\sim$34% and a time scale of days.

IV. DISCUSSION

In summary, out of a total of 12 stars in our sample, four stars (namely Cyg–OB2 8A, ζ Pup, δ Ori, and 15 Mon) exhibit count rate variations between different data sections at different effective amplitude and significance level. Only one star (τ Sco) exhibits marginal short-term variability with an effective amplitude of $\sim$30% and a time scale of $\sim$50 s. For the other stars in our sample the short-term variability analysis gives upper limits in the range $\sim$10%–30%, somewhat compatible with the variability observed in τ Sco (see Table 3).

Only long-term variability has been detected unam-

biguously (i.e., with a very high significance level). The quoted time scale of these long-term variations is deduced by the separation between different data sections and could be unrelated to the actual pattern of the source time variability, pattern that in no case has been observed. The light curve of Cyg–OB2 8A (Fig. 1), the star with the best statistics in our sample and whose observation spans several hundred kiloseconds with a good (compared to the other variable stars in the sample) effective coverage of the span interval, tentatively suggests the existence of two different emission levels; the emission at each level lasts hundreds of kiloseconds. All of the long-term variability detected, as well as the data available for the "constant" sources in our sample are compatible with a similar variability pattern. Our long-term variability analysis confirms the previous findings, based on partially different data sets, of Snow, Cash, and Grady (1981) that 15 Mon and δ Ori are variable. ι Ori does not show variability in our data.

The observation of X-ray variability over time scales of several hours in OB stars is consistent with previous observations in different wave-bands (see Henrichs 1988 and references therein). Variability in UV lines of OB stars is generally interpreted in terms of variations occurring in the wind of these stars (for a review see Henrichs 1988). We note that the detected long-term variability is mainly characteristic of the soft energy band and can therefore be easily accounted for by any model allowing a modulation in the absorbing medium. For this reason it is difficult to use these results to constrain models, since in order to do this we would need synoptic observations as well as a coherent theory which ties line flux variations to soft X-ray variations (which does not as yet exist). In this respect, the short-term variability analysis of hard and total energy bands is much more constraining.

Short-term variability was detected only in τ Sco although only marginally, while the effective variability of all other stars in the sample is below 10%–20%. This result implies an emission mechanism able to generate a stationary (at least up to our sensitivity threshold) X-ray flux on time scales from few tens of seconds up to $\sim$1 hr. If one considers shock models (Lucy and White 1980; Lucy 1982; Cassinelli and Swank 1983; Owocki and Rybicki 1985; Baade and Lucy 1987), a straightforward implication is that the number of shocks responsible for the X-ray emission is large (i.e., $\gtrsim 10$) since their formation and dissipation do not produce detectable flux variations, or the shocks are long-lived so that their total number does not change during our observations, or both. The variability observed in τ Sco seems to be the exception rather than the rule; a possible explanation could be that variability in OB stars normally occurs with an amplitude distribution that leaves the bulk of variations below the sensitivity threshold and allows the detection of the largest events only. These events would then have been detected by chance in τ Sco but in principle could have been detected in any of the other stars in the sample. This interpretation would imply, in the framework of shock models, a quenching or steepening mechanism capable to dissipate shocks and produce variability on time scales as short as 50 s.

An alternative possibility is that X-ray variability is peculiar of τ Sco only while the other stars in the sample emit a constant flux. We note that X-ray and bolometric luminosities, mass-loss rates, and terminal wind velocities span several order of magnitudes for the stars in our sample, and hence one would not expect an homogeneous behavior of the X-ray emission. The sample is however far too small to allow a meaningful correlation study between X-ray properties and other physical parameters.

Do our results exclude any of the other competing models for soft X-ray production in OB stars (viz., Rosner and Vaiana 1979; Cassinelli *et al.* 1981; Stewart and Fabian 1981; Waldron 1982, 1984; Krolik and Raymond 1985)? In these cases, we believe that better observational constraints can derive from future observations; fluctuations in the "hard band" are in fact decisive in discriminating between models (since "soft band" fluctuations can be accounted for by modulations in the absorbing medium). While our data are compatible with such fluctuations and there is indeed some rather scanty evidence of their existence, the sensitivity achieved with the present data does not allow us to draw a definitive conclusion.

We would like to acknowledge support of the Italian Ministry for Public Education, and National Research Council (PSN), and NASA grants NAG 8-445 and NAS8-30751; A. C. and S. Serio would also like to thank the support of the Smithsonian Institution Visitors Program.

REFERENCES

Baade, D., and Lucy, L. B. 1987, *Astr. Ap.*, **178**, 213.
Cassinelli, J. P., Hartmann, L., Sanders, W. T., Dupree, A. K., and Myers, R. V. 1983, *Ap. J.*, **268**, 205.
Cassinelli, J. P., and Swank, J. H. 1983, *Ap. J.*, **271**, 681.
Cassinelli, J. P., Waldron, W. L., Sanders, W. T., Harnden, F. R. Jr., Rosner, R., and Vaiana, G. S. 1981, *Ap. J.*, **250**, 677.
Chlebowsky, T., Harnden, F. R., Jr., and Sciortino, S. 1988, *Ap. J.*, submitted.
Collura, A., Maggio, A., Sciortino, S., Serio, S., Vaiana, G. S., and Rosner, R. 1987, *Ap. J.*, **315**, 340.
Eadie, W. T., Drijard, D., James, F. E., Ross, M., and Sadoulet, B. 1971, *Statistical Methods in Experimental Physics* (Dordrecht: North-Holland).
Giacconi, R., *et al.* 1979, *Ap. J.*, **230**, 540.
Gorenstein, P., Harnden, F. R., Jr., and Fabricant, D. G. 1981, *IEEE Trans. Nucl. Sci.*, **NS-28**, 869.
Gry, C., Lamers, H. J. G. L. M., and Vidal-Madjar, A. 1984, *Astr. Ap.*, **137**, 29.
Harnden, F. R., Jr., Branduardi, G., Elvis, M., Gorenstein, P., Grindlay, J., Pye, J. P., Rosner, R., Topka, K., and Vaiana, G. S. 1979, *Ap. J.* (*Letters*), **234**, L51.
Harnden, F. R. Jr., Fabricant, D. G., Harris, D. E., and Schwarz, J. 1984, *SAO Spec. Rept.*, No. 393.
Harnden, F. R. Jr., Vaiana, G. S., Sciortino, S., Micela, G., Maggio, A., Schmitt, J. H. M. M., and Rosner, R. 1989, in preparation.
Henrichs, H. 1988, in *O, Of, and Wolf-Rayet Stars*, ed. P. S. Conti and A. B. Underhill (NASA/CNRS Monograph), in press.
Krolik, J. H., and Raymond, C. J., 1985, *Ap. J.*, **298**, 660.
Long, K. S., and White, R. L. 1980, *Ap. J.* (*Letters*), **239**, L65.
Lucy, L. B. 1982, *Ap. J.*, **255**, 286.
Lucy, L. B., and White, R. L. 1980, *Ap. J.*, **241**, 300.
Owocki, S., and Rybicki, G. 1985, *Ap. J.*, **29**, 265.
Prinja, R. K., and Howart, I. D. 1986, *Ap. J. Suppl.*, **61**, 357.
Rosner, R., and Vaiana, G. S. 1979, in *X-Ray Astronomy*, ed. R. Giacconi and G. Setti (Dordrecht: Reidel).
Seward, F. D., and Chlebowski, T. 1982, *Ap. J.*, **256**, 530.
Seward, F. D., Forman, W. R., Giacconi, R., Griffiths, R. E., Harnden, F. R. Jr., Jones, C., and Pye, J. P. 1979, *Ap. J.* (*Letters*), **234**, L55.
Snow, T. P., Jr., Cash, W., and Grady, C. A. 1981, *Ap. J.* (*Letters*), **244**, L19.

Stewart, G. C., and Fabian, A. 1981, *M.N.R.A.S.*, **197**, 713.
Vaiana, G. S., *et al.* 1981, *Ap. J.*, **245**, 312.
Vidal-Madjar, A., Laurent, C., Gry, C., Bruston, P., Ferlet, R., and York, D. G. 1983, *Astr. Ap.*, **120**, 58.
Waldron, W. 1982, Ph.D. thesis, University of Wisconsin, Madison.
———. 1984, *Ap. J.*, **282**, 256.
York, D. G., Vidal-Madjar, A., Laurent, C., and Bonnet, R. 1977, *Ap. J. (Letters)*, **213**, L67.

A. COLLURA: Istituto per le Applicazioni Interdisciplinari della Fisica, (I.A.I.F)–National Research Council, Via Archirafi 36, 90136 Palermo, Italy

F. R. HARNDEN, JR.: Harvard-Smithsonian Center for Astrophysics, 60 Garden Street, Cambridge, MA 02138

R. ROSNER: Department of Astronomy and Astrophysics, The University of Chicago, 5640 South Ellis Avenue, Chicago, IL 60637

S. SCIORTINO, S. SERIO, and G. S. VAIANA: Osservatorio Astronomico, Palazzo dei Normanni, 90134 Palermo, Italy